

# Singularities in ground-state fidelity and quantum phase transitions for the Kitaev model

Jian-Hui Zhao and Huan-Qiang Zhou

*Department of Physics and Centre for Modern Physics, Chongqing University, Chongqing 400044, People's Republic of China*

(Received 23 December 2008; revised manuscript received 10 March 2009; published 1 July 2009)

The ground-state fidelity per lattice site is shown to be able to detect quantum phase transitions for the Kitaev model on the honeycomb lattice, a prototypical example of quantum lattice systems with topological order. It is found that, in the thermodynamic limit, the ground-state fidelity per lattice site is nonanalytic at the phase boundaries; the second-order derivative of its logarithmic function with respect to a control parameter describing the interaction between neighboring spins is divergent. A finite-size scaling analysis is performed, which allows us to extract the correlation length critical exponent from the scaling behaviors of a part of the ground-state fidelity per lattice site.

DOI: [10.1103/PhysRevB.80.014403](https://doi.org/10.1103/PhysRevB.80.014403)

PACS number(s): 75.10.Jm, 05.70.Jk, 03.67.—a

## I. INTRODUCTION

With the advent of its discovery in the fractional quantum-Hall effect,<sup>1</sup> topological order emerges as a new paradigm in the study of quantum phase transitions (QPTs).<sup>2</sup> Subsequent investigations show that topological order occurs in various strongly correlated lattice systems undergoing QPTs. A characteristic feature of quantum systems with topological order is their insensitivity to any *local* perturbations.<sup>3</sup> Such an essential difference between topological and symmetry-breaking orders invalidates the usual tools used to describe a symmetry-breaking order, such as long-range correlations, broken symmetries, and local order parameters.<sup>4,5</sup>

Recently, much attention has been paid to an exactly solvable spin-1/2 model on a honeycomb lattice introduced by Kitaev<sup>5</sup> for fault-tolerant topological quantum computation.<sup>6</sup> The model describes a set of spins located at the vertices of a two-dimensional honeycomb lattice, subject to a spatially anisotropic interaction between neighboring spins. It has been shown that it carries excitations with both Abelian and non-Abelian braiding statistics, which do not obey ordinary bosonic and fermionic statistics but are anyons with more intricate statistical behavior.<sup>7</sup> An experimentally feasible realization of the model in a system of cold atoms on an optical lattice has been addressed<sup>8</sup> (see also Refs. 9 and 10) with the expectation to perform quantum computation by utilizing braiding of collective excitations implanted in topologically ordered coherent quantum many-body states.

In addition, a viable scheme to determine the ground-state phase diagram of a quantum lattice system without prior knowledge of order parameters was proposed in Refs. 11–14. This was achieved by studying the singularities in the ground-state fidelity per lattice site.<sup>15</sup> In fact, the ground-state fidelity may be interpreted as the partition function of a classical statistical vertex model with the same lattice geometry by using the tensor-network representations of quantum many-body wave functions.<sup>12</sup> Therefore, the fidelity per lattice site is nothing but the partition function per site in the classical statistical vertex lattice model.<sup>16</sup> This justifies why QPTs may be detected as singularities in the fidelity per lattice site as a function of the control parameters (see also Refs. 17 and 18 for the connection between the fidelity and

QPTs). Therefore, an intriguing question is to see if the fidelity approach captures the physics underlying QPTs in quantum lattice systems with topological order.

The purpose of this paper is to show that the ground-state fidelity per lattice site is able to detect QPTs for the Kitaev model on the honeycomb lattice, a prototypical example of quantum lattice systems with topological order. First, we derive the ground-state fidelity per lattice site between different ground states from the exact solution of the Kitaev model on the honeycomb lattice. This is achieved by exploiting the fact that the original spin model on the honeycomb lattice is rephrased as a *p*-wave BCS model with a site-dependent chemical potential for spinless fermions on a square lattice<sup>19</sup> (see also Refs. 20–23). The ground state of the latter is a BCS-type state, as a consequence of the Jordan-Wigner, Fourier, and Bogoliubov transformations. Second, the phase boundaries separating the gapless phase from different gapful phases are reproduced by investigating the singularities in the fidelity per lattice site. It is found that, in the thermodynamic limit, the ground-state fidelity per site is nonanalytic at the phase boundaries. That is, the second-order derivative of its logarithmic function with respect to a given control parameter is divergent as the phase boundaries are crossed. Third, we perform a finite-size scaling analysis for the Kitaev model, aiming at extracting the correlation length critical exponent from the scaling behaviors of the ground-state fidelity per site. Our exact results offer a benchmark to investigate QPTs for two-dimensional quantum lattice systems with topological order numerically in the context of tensor-network representations.<sup>24–27</sup>

## II. KITAEV MODEL ON A HONEYCOMB LATTICE

Consider a spin 1/2 model on a honeycomb lattice with the Hamiltonian<sup>1</sup>

$$H = -J_x \sum_{x\text{-bonds}} \sigma_i^x \sigma_j^x - J_y \sum_{y\text{-bonds}} \sigma_i^y \sigma_j^y - J_z \sum_{z\text{-bonds}} \sigma_i^z \sigma_j^z, \quad (1)$$

where  $J_\alpha$  are interaction (control) parameters and  $\sigma_j^\alpha$  are the Pauli matrices at the site  $j$  with  $\alpha=x, y, \text{ and } z$ . The Hamiltonian (1) may be fermionized by performing the Jordan-Wigner transformation<sup>19–22</sup> from the Pauli spin matrices  $\sigma_j^\alpha$  to the spinless-fermion operators  $c_j^\dagger$  and  $c_j$ . This one-

dimensional fermionization is realized by deforming the hexagonal lattice into a brick-wall lattice which is topologically equivalent to the original lattice. Following Chen and Nussinov,<sup>19</sup> we introduce the Majorana fermions:  $A_{w(b)} = (c_{w(b)} - c_{w(b)}^\dagger)/i$  and  $B_{w(b)} = c_{w(b)} + c_{w(b)}^\dagger$ . Then the Hamiltonian (1) becomes

$$H = -iJ_x \sum_{x\text{-bonds}} A_w A_b + iJ_y \sum_{y\text{-bonds}} A_b A_w - iJ_z \sum_{z\text{-bonds}} \alpha_r A_b A_w, \quad (2)$$

where the subscripts  $w$  and  $b$  denote two sublattices in the brick-wall lattice, and  $\alpha_r \equiv iB_b B_w$  along the  $z$  bond is conserved,<sup>20</sup> with  $r$  being the coordinate of the midpoint of the bond connecting the  $b$ -type and  $w$ -type sites. This in turn is equivalent to a model of spinless fermions on a square lattice with a site-dependent chemical potential

$$H = J_x \sum_r (d_r^\dagger + d_r)(d_{r+\hat{x}}^\dagger - d_{r+\hat{x}}) + J_y \sum_r (d_r^\dagger + d_r)(d_{r+\hat{y}}^\dagger - d_{r+\hat{y}}) + J_z \sum_r \alpha_r (2d_r^\dagger d_r - 1). \quad (3)$$

Here  $d = (A_w + iA_b)/2$  and  $d^\dagger = (A_w - iA_b)/2$ , and the unit vector  $\hat{e}_x$  and  $\hat{e}_y$  connects two  $z$  bonds and crosses  $x$  and  $y$  bonds, respectively. For large enough systems, the ground-state configurations are bulk vortex-free configurations,<sup>1,21</sup> which implies  $\alpha_r = 1$  for all  $r$ . Therefore, the ground state may be obtained by performing a Fourier transformation. Up to an unimportant additive constant, Hamiltonian (3) in the vortex-free configuration now reads as

$$H_g = \sum_k \left[ \epsilon_k d_k^\dagger d_k + i \frac{\Delta_k}{2} (d_k^\dagger d_{-k}^\dagger - \text{H.c.}) \right] \quad (4)$$

with  $\epsilon_k = 2J_z - 2J_x \cos k_x - 2J_y \cos k_y$  and  $\Delta_k = 2J_x \sin k_x + 2J_y \sin k_y$ . Hamiltonian (4) is a  $p$ -wave-type BCS pairing model and can be diagonalized by means of the Bogoliubov transformation. It yields that the BCS-type ground state is  $|g\rangle = \prod_k (u_k + v_k d_k^\dagger d_{-k}^\dagger) |0\rangle$ , where  $|u_k|^2 = 1/2(1 + \epsilon_k/E_k)$  and  $|v_k|^2 = 1/2(1 - \epsilon_k/E_k)$  with the quasiparticle excitation energy  $E_k = \sqrt{\epsilon_k^2 + \Delta_k^2}$ .<sup>19</sup> We choose the phase convention  $u_k = \sqrt{(E_k + \epsilon_k)/2E_k}$  and  $v_k = i\Delta_k/\sqrt{2E_k^2 + 2E_k\epsilon_k}$  for later uses.

### III. GROUND-STATE FIDELITY PER LATTICE SITE

Consider two ground states  $|g\rangle$  and  $|g'\rangle$  corresponding to different values of the control parameters  $\vec{J} \equiv (J_x, J_y, J_z)$  and  $\vec{J}' \equiv (J'_x, J'_y, J'_z)$ , respectively. The fidelity  $F(\vec{J}; \vec{J}') \equiv \langle g' | g \rangle$  asymptotically scales as  $F(\vec{J}; \vec{J}') \sim d(\vec{J}; \vec{J}')^N$ , with  $N$  as the total number of sites in the lattice. Here  $d(\vec{J}; \vec{J}')$  is the ground-state fidelity per lattice site, introduced in Refs. 11 and 12. Although  $F(\vec{J}; \vec{J}')$  becomes trivially zero for continuous QPTs, the fidelity per lattice site is well defined in the thermodynamic limit

$$d(\vec{J}; \vec{J}') = \lim_{N \rightarrow \infty} F^{1/N}(\vec{J}; \vec{J}'). \quad (5)$$

It satisfies the properties inherited from the fidelity  $F(\vec{J}; \vec{J}')$ : (i) normalization  $d(\vec{J}; \vec{J}) = 1$ , (ii) symmetry  $d(\vec{J}; \vec{J}') = d(\vec{J}'; \vec{J})$ , and (iii) range  $0 \leq d(\vec{J}; \vec{J}') \leq 1$ .

For the Kitaev model on the honeycomb lattice, the logarithmic function of the fidelity per site,  $\ln d_h(\vec{J}; \vec{J}')$ , is half of the logarithmic function of the fidelity per site,  $\ln d_{\text{sq}}(\vec{J}; \vec{J}')$ , for the model of spinless fermions on a square lattice. This results from the fact that the number of sites in the honeycomb lattice doubles that of sites in the square lattice. The BCS-type ground state  $|g\rangle$  yields the ground-state fidelity per lattice site for the spinless-fermion model on the square lattice

$$\ln d_{\text{sq}}(\vec{J}; \vec{J}') = \frac{1}{(2\pi)^2} \int_{-\pi}^{\pi} dk_x \int_0^{\pi} dk_y \ln(u_k^* u'_k + v_k^* v'_k), \quad (6)$$

where  $u_k$  and  $v_k$  depend on  $\vec{J}$ , whereas  $u'_k$  and  $v'_k$  depend on  $\vec{J}'$ . Here we emphasize that although the information about the topological nature of the Kitaev model is lost in the spinless-fermion representation, the unitary equivalence between the two representations preserves the fidelity. Since the extra prefactor does not affect the singularities in  $\ln d_h(\vec{J}; \vec{J}')$  and  $\ln d_{\text{sq}}(\vec{J}; \vec{J}')$ , hereafter we focus on  $\ln d_{\text{sq}}(\vec{J}; \vec{J}')$ .

For a finite-size system, Hamiltonian (4), resulted from the Jordan-Wigner, Fourier, and Bogoliubov transformations, depends on boundary conditions imposed on the original spin model [Eq. (1)]. In contrast to open boundary conditions, there is an extra boundary term if one adopts the periodic boundary conditions. However, such a boundary term does not contribute to the fidelity per site although it carries the topological dependence of the ground-state degeneracy.<sup>19</sup> From now on, we are only concerned with the fermion model on a square lattice with the periodic boundary conditions (i.e., a torus) to analyze the ground-state fidelity per lattice site for finite-size systems,<sup>28</sup> from which it is sufficient to extract the bulk behaviors of the model. As such, for a system on a torus with an odd linear size  $L$ , the logarithmic function of the ground-state fidelity per lattice site,  $\ln d_{\text{sq}}(\vec{J}; \vec{J}')$ , takes the form

$$\ln d_{\text{sq}}(\vec{J}; \vec{J}') = \frac{1}{L^2} \sum_{k_x, k_y} \ln(u_k^* u'_k + v_k^* v'_k). \quad (7)$$

Here  $k_x$  and  $k_y$  take values from the set:  $2\pi m/L [m = -(L-1)/2, \dots, (L-1)/2]$  and the double summation is over all  $k_x$  and the positive values of  $k_y$ .

#### A. Ground-state phase diagram and singularities in the ground-state fidelity per lattice site

Now we turn to the ground-state phase diagram. This follows from the singularities in  $\ln d(\vec{J}; \vec{J}')$ . From now on, the subscript “sq” has been omitted for brevity. One may show that  $\ln d(\vec{J}; \vec{J}')$  in Eq. (6) and the first-order derivative with respect to a control parameter is continuous but the second-

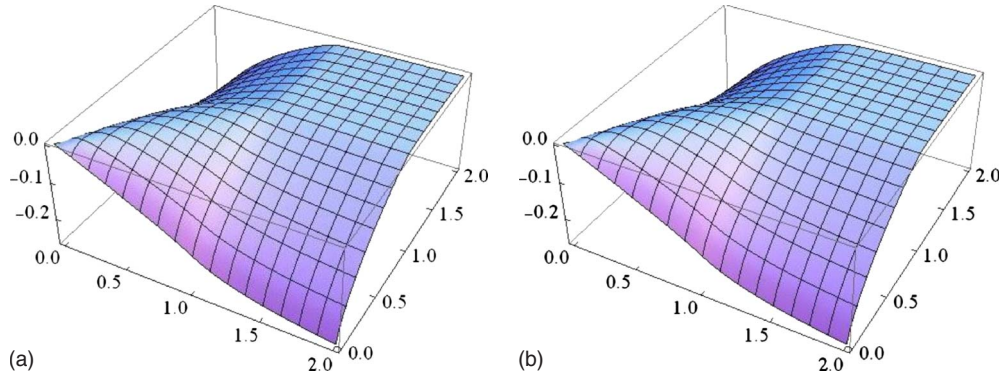


FIG. 1. (Color online) (a) The logarithm of the fidelity per lattice site,  $\ln d(\vec{J}; \vec{J}')$ , is shown as a function of  $J_x$  and  $J'_x$  for fixed  $J_y=J'_y=J_z=J'_z=1/2$ . It exhibits a pinch point at  $(J_{xc}, J_{xc})=(1, 1)$ . (b) The logarithm of the fidelity per lattice site,  $\ln d(\vec{J}; \vec{J}')$ , is shown as a function of  $J_z$  and  $J'_z$  for fixed  $J_x=J'_x=J_y=J'_y=1/2$ . It exhibits a pinch point at  $(J_{zc}, J_{zc})=(1, 1)$ . We see that they are identical. That is, the ground state fidelity per lattice site,  $d(\vec{J}; \vec{J}')$ , captures the fact that the Kitaev model is symmetric in  $J_x$ ,  $J_y$ , and  $J_z$ . Here, a pinch point is defined as an intersection of two singular lines.

order derivative diverges when the phase boundaries determined by  $|J_x|=|J_y|+|J_z|$ ,  $|J_y|=|J_z|+|J_x|$ , and  $|J_z|=|J_x|+|J_y|$  are crossed. This is consistent with the original analysis by Kitaev<sup>1</sup> (see also Refs. 19–21). Indeed, the Kitaev model is symmetric in  $J_x$ ,  $J_y$ , and  $J_z$ . Therefore, this should be reflected in all physical quantities including the fidelity per lattice site. However, the mapping from the Kitaev model on the honeycomb lattice to the spinless-fermion model on the square lattice makes this fact a bit obscure. To check the symmetry, we compute the logarithm of the ground-state fidelity per lattice site for two cases: (i)  $J_y=J'_y=J_z=J'_z=1/2$  as a function of  $J_x, J'_x$  and (ii)  $J_x=J'_x=J_y=J'_y=1/2$  as a function of  $J_z, J'_z$ . In Fig. 1(a), we plot  $\ln d(\vec{J}; \vec{J}')$  as a function of  $J_x$  and  $J'_x$  for  $J_y=J_z=1/2$  and  $J'_y=J'_z=1/2$ . It exhibits a pinch point at  $(J_{xc}, J_{xc})=(1, 1)$ . In Fig. 1(b), we plot  $\ln d(\vec{J}; \vec{J}')$  as a function of  $J_z$  and  $J'_z$  for fixed  $J_x=J'_x=J_y=J'_y=1/2$ . It exhibits a pinch point at  $(J_{zc}, J_{zc})=(1, 1)$ . Here by a pinch point we mean an intersection of two singular lines  $J_x=J_{xc}$  and  $J'_x=J_{xc}$ . Therefore, the drastic change in the ground-state many-body wave functions at a critical point is reflected as the singularities in  $\ln d(\vec{J}; \vec{J}')$ . We see that  $\ln d(\vec{J}; \vec{J}')$  is identical for both cases, indicating that the symmetry is captured by the ground-state fidelity per lattice site  $d(\vec{J}; \vec{J}')$ .

### B. Singularities in a part of the ground-state fidelity per lattice site

In fact,  $\ln d(\vec{J}; \vec{J}')$  consists of two parts:  $\ln d_{++}(\vec{J}; \vec{J}')$  and  $\ln d_{--}(\vec{J}; \vec{J}')$ . The former is the contribution from the positive values of  $k_x$  and  $k_y$ , whereas the latter is the contribution from the negative values of  $k_x$  and the positive values of  $k_y$ . Since the singularities in  $\ln d(\vec{J}; \vec{J}')$  come from both parts, we restrict ourselves to consider  $\ln d_{++}(\vec{J}; \vec{J}')$ . In Fig. 2(a), we plot  $\ln d_{++}(\vec{J}; \vec{J}')$  as a function of  $J_x$  and  $J'_x$  for  $J_y=J_z=1/2$  and  $J'_y=J'_z=1/2$ . It is seen that a pinch point occurs at  $(J_{xc}, J_{xc})=(1, 1)$ . Similarly, the numerical results are plotted in Fig. 2(b) for  $\ln d_{++}(\vec{J}; \vec{J}')$  as a function of  $J_z$  and  $J'_z$  for fixed  $J_x=J'_x=J_y=J'_y=1/2$  with a pinch point at  $(J_{zc}, J_{zc})=(1, 1)$ . Not surprisingly, the symmetry mentioned above for the Kitaev model with respect to  $J_x$ ,  $J_y$ , and  $J_z$  is lost for  $\ln d_{++}(\vec{J}; \vec{J}')$ , although it is valid for  $\ln d(\vec{J}; \vec{J}')$ . The reason why we investigate  $\ln d_{++}(\vec{J}; \vec{J}')$  is that it considerably simplifies the finite-size scaling analysis without loss of any physics. This is because there is only an isolated singular point (0,0) in the momentum space  $(k_x, k_y)$  for  $\ln d_{++}(\vec{J}; \vec{J}')$ . Instead, a singular line in the momentum space  $(k_x, k_y)$  occurs for  $\ln d_{sq}(\vec{J}; \vec{J}')$ .

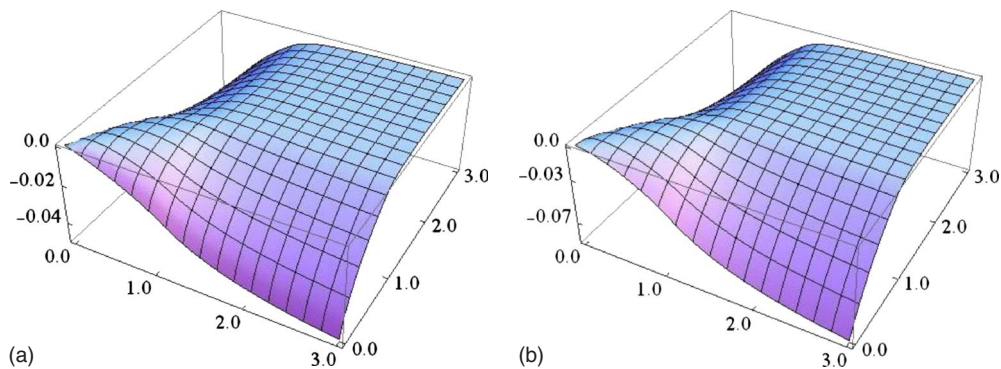


FIG. 2. (Color online) (a) A part of the logarithm of the fidelity per lattice site,  $\ln d_{++}(\vec{J}; \vec{J}')$ , is shown as a function of  $J_x$  and  $J'_x$  for fixed  $J_y=J'_y=J_z=J'_z=1/2$ . It exhibits a pinch point at  $(J_{xc}, J_{xc})=(1, 1)$ . (b) A part of the logarithm of the fidelity per lattice site,  $\ln d_{++}(\vec{J}; \vec{J}')$ , is shown as a function of  $J_z$  and  $J'_z$  for fixed  $J_x=J'_x=J_y=J'_y=1/2$ . It exhibits a pinch point at  $(J_{zc}, J_{zc})=(1, 1)$ .

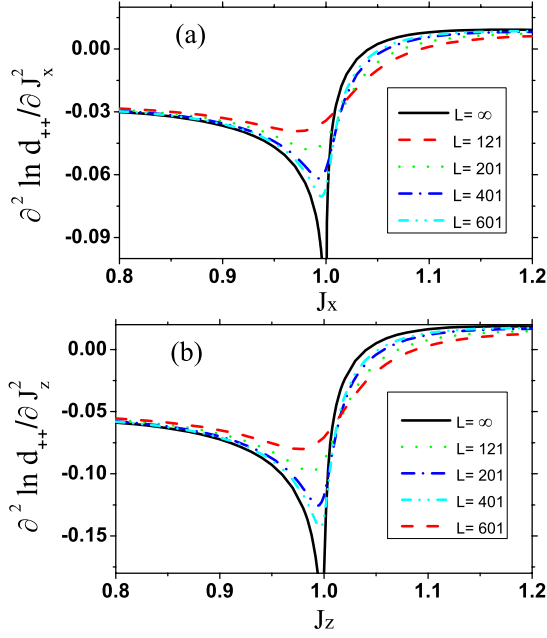


FIG. 3. (Color online) (a) The second-order derivative of a part of the logarithm of the fidelity per lattice site,  $\ln d_{++}(\vec{J}, \vec{J}')$ , with respect to  $J_x$  diverges at the critical point in the thermodynamic limit. However, it remains analytic for finite-size systems, although more pronounced dips occur with increasing linear system size. Here  $J'_x=0.8$  and  $J_y=J'_y=J_z=J'_z=1/2$ . (b) The second-order derivative of a part of the logarithm of the fidelity per lattice site,  $\ln d_{++}(\vec{J}, \vec{J}')$ , with respect to  $J_z$  diverges at the critical point in the thermodynamic limit. However, it remains analytic for finite-size systems, although more pronounced dips occur with increasing linear system size. Here  $J'_z=0.8$  and  $J_x=J'_x=J_y=J'_y=1/2$ .

More precisely, for any fixed  $\vec{J}'$ ,  $\ln d_{++}(\vec{J}; \vec{J}')$  is logarithmically divergent when  $\vec{J}'$  is varied such that a critical point is crossed. Suppose  $J_y$  and  $J_z$  are fixed and only  $J_x$  is a control parameter that varies. Then we have

$$\frac{\partial^2 \ln d_{++}(\vec{J}, \vec{J}')}{\partial J_x^2} = k_1 \ln |J_x - J_{xc}| + \text{const}, \quad (8)$$

where  $k_1$  is a nonuniversal prefactor that depends on  $J_y$ ,  $J_z$ , and  $\vec{J}'$ , and  $J_{xc}$  is the critical value of  $J_x$  for fixed  $J_y$  and  $J_z$ . The numerical results are plotted in Fig. 3(a) for  $J_y=J_z=1/2$  and  $J_{xc}=1$ . The least square fit yields  $k_1 \approx 0.02360$ , which is close to the analytical result:  $k_1 = 1/(4\pi^2)$ . We stress that an estimation of  $k_1$  is getting closer to the analytical prediction if the fitting interval gets smaller. Similarly, we have presented numerics in Fig. 3(b) for the second-order derivative of  $\ln d_{++}(\vec{J}; \vec{J}')$  with respect to  $J_z$  with  $J'_z=0.8$  and  $J_x=J'_x=J_y=J'_y=1/2$ . It turns out that it diverges logarithmically in the same way as Eq. (8) with  $J_x$  replaced by  $J_z$  and  $k_1 \approx 0.04726$ . The analytical prediction is  $k_1 = 1/(2\pi^2)$ .<sup>29</sup>

### C. Finite-size scaling analysis

For a system of finite size  $N \equiv L^2$  (with  $L$  the linear size), there is no divergence in the second-order derivative of  $\ln d_{++}(\vec{J}, \vec{J}')$  with respect to  $J_x$  since QPTs only occur in the

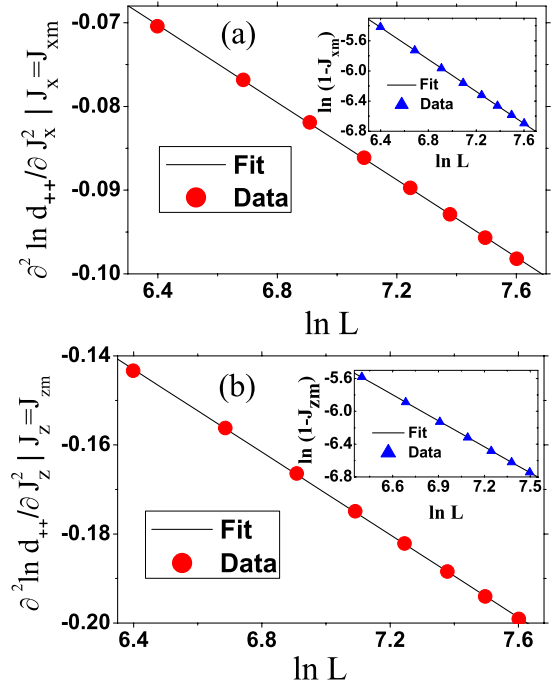


FIG. 4. (Color online) (a) Main: the dips values scale as  $\ln L$  with increasing linear size  $L$  for  $J'_x=0.8$  and  $J_y=J'_y=J_z=J'_z=1/2$ . Inset: the positions of the dips, i.e., the quasicritical points,  $J_{xm}$ , approach the critical point  $J_{xc}=1$  with increasing linear size  $L$ . (b) Main: the dips values scales as  $\ln L$  with the linear size  $L$  for  $J'_z=0.8$  and  $J_x=J'_x=J_y=J'_y=1/2$ . Inset: the positions of the dips,  $J_{zm}$ , approach the critical point  $J_{zc}=1$  with increasing linear size  $L$ .

thermodynamic limit. Instead, as seen in Fig. 3(a), some pronounced dips occur at the so-called quasicritical points  $J_{xm}$  with the dips values logarithmically diverging with increasing linear size  $L$

$$\frac{\partial^2 \ln d_{++}(\vec{J}, \vec{J}')}{\partial J_x^2} \Big|_{J_x=J_{xm}} = k_2 \ln L + \text{const}, \quad (9)$$

where  $k_2$  is a nonuniversal prefactor  $k_2$ , which takes the value  $k_2 \approx -0.02312$  for  $J'_x=0.8$  and  $J_y=J'_y=J_z=J'_z=1/2$  [see Fig. 4(a)]. In addition, the pseudocritical point  $J_{xm}$  approaches the critical value as  $J_{xm} \sim 1 - 3.96384L^{-1.06245}$  [see the inset in Fig. 4(a)]. The scaling ansatz in the system exhibiting logarithmic divergences requires that the absolute value of the ratio  $k_1/k_2$  is the correlation length critical exponent  $\nu$ . In this case,  $|k_1/k_2| \sim 1.02076$ , very close to the exact value  $\nu=1$ . This is consistent with the fact that the gap  $\Delta$  for the Bogoliubov quasiparticle scales as  $\Delta \sim J_x - J_{xc}$  near the critical point  $J_{xc}$ . Similarly, a finite-size scaling analysis is performed for  $\ln d_{++}(\vec{J}, \vec{J}')$  with  $J'_z=0.8$  and  $J_x=J'_x=J_y=J'_y=1/2$ . It yields  $k_2 \approx -0.04640$  for  $\partial^2 \ln d_{++}(\vec{J}, \vec{J}') / \partial J_z^2|_{J_z=J_{zm}}$  [see Fig. 4(b)] and the pseudocritical point  $J_{zm}$  are plotted in the inset in Fig. 4(b).

In order to address the scaling ansatz for a system exhibiting logarithmic divergence,<sup>30</sup> we take into account the distance of the minimum of  $\partial^2_{J_x} \ln d_{++}(\vec{J}, \vec{J}')$  from the critical point to investigate  $D(\vec{J}, \vec{J}') \equiv 1 - \exp[\partial^2_{J_x} \ln d_{++}(\vec{J}, \vec{J}')$

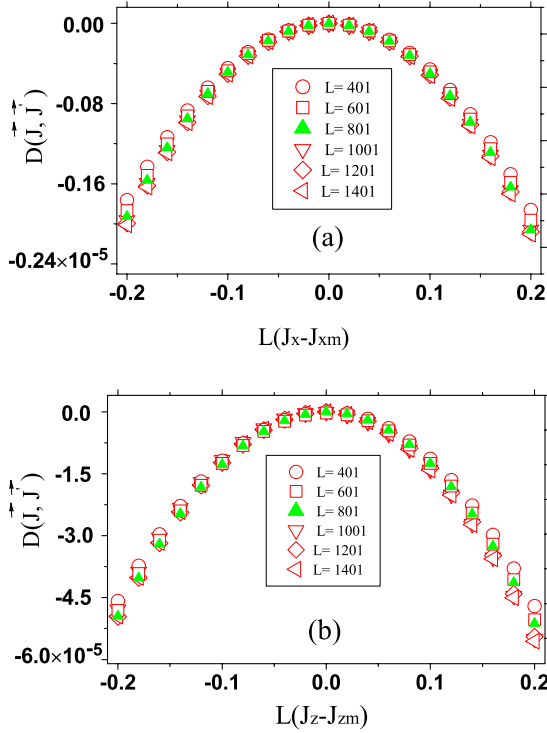


FIG. 5. (Color online) (a) A finite-size scaling analysis is performed for a quantity defined as  $D(\vec{J}, \vec{J}') \equiv 1 - \exp[\partial_{J_x}^2 \ln d_{++}(\vec{J}, \vec{J}') - \partial_{J_x}^2 \ln d_{++}(\vec{J}, \vec{J}')|_{J_x=J_{xm}}]$ , with  $J_y$ ,  $J_z$ , and  $\vec{J}'$  fixed. The scaling ansatz for logarithmic divergences implies that  $D(\vec{J}, \vec{J}')$  is a function of  $L(J_x - J_{xm})$  for fixed  $J_y$ ,  $J_z$ , and  $\vec{J}'$ . (b) A finite-size scaling analysis is performed for a quantity defined as  $D(\vec{J}, \vec{J}') = 1 - \exp[\partial_{J_z}^2 \ln d_{++}(\vec{J}, \vec{J}') - \partial_{J_z}^2 \ln d_{++}(\vec{J}, \vec{J}')|_{J_z=J_{zm}}]$ , with  $J_x$ ,  $J_y$ , and  $\vec{J}'$  fixed. The scaling ansatz implies that  $D(\vec{J}, \vec{J}')$  is a function of  $L(J_z - J_{zm})$  for fixed  $J_x$ ,  $J_y$ , and  $\vec{J}'$ . All the data from  $L=401$  up to  $L=1401$  collapse onto a single curve. This shows that the system at a critical point is scale invariant and that the correlation length critical exponent  $\nu$  is 1.

$-\partial_{J_x}^2 \ln d_{++}(\vec{J}, \vec{J}')|_{J_x=J_{xm}}]$  as a function of  $L(J_x - J_{xm})$  for different linear sizes  $L$ 's. The numerical results for the linear size ranging from  $L=401$  up to  $L=1401$  are plotted in Fig. 5(a). All the data for different  $L$ 's collapse onto a single curve, indicating that the model is scale invariant, i.e.,  $\xi/L = \xi'/L'$ , and that the correlation length critical exponent  $\nu = 1$ . The same conclusion can be drawn from Fig. 5(b), where the data collapsing is confirmed for  $1 - \exp[\partial_{J_z}^2 \ln d_{++}(\vec{J}, \vec{J}') - \partial_{J_z}^2 \ln d_{++}(\vec{J}, \vec{J}')|_{J_z=J_{zm}}]$ .

#### IV. SUMMARY

We have demonstrated that the ground-state fidelity per lattice site is able to detect QPTs in the Kitaev model on the honeycomb lattice. It is found that, in the thermodynamic limit, the ground-state fidelity per lattice site is nonanalytic at a critical point. A finite-size scaling analysis has also been performed to extract the correlation length critical exponent from the scaling behaviors of (a part of) the ground-state fidelity per site. Our exact results offer a benchmark to numerically investigate QPTs for two-dimensional quantum lattice systems with topological order in the context of tensor-network algorithms, which is currently under investigation.

#### ACKNOWLEDGMENTS

We thank Yupeng Wang for insightful discussions about the Kitaev model and comments on the manuscript. This work is supported in part by the National Natural Science Foundation of China (Grants No. 10774197 and No. 10874252) and the Natural Science Foundation of Chongqing (Grant No. CSTC, 2008BC2023).

- <sup>1</sup>D. C. Tsui, H. L. Stormer, and A. C. Gossard, Phys. Rev. Lett. **48**, 1559 (1982).
- <sup>2</sup>X.-G. Wen, *Quantum Field Theory of Many-Body Systems* (Oxford University Press, Oxford, 2004).
- <sup>3</sup>Z. Nussinov and G. Ortiz, arXiv:cond-mat/0702377 (unpublished).
- <sup>4</sup>However, the existence of a mapping from a system with topological order to a system with symmetry-breaking order is possible, as shown for the Kitaev model (Ref. 20).
- <sup>5</sup>A. Kitaev, Ann. Phys. **321**, 2 (2006).
- <sup>6</sup>A. Yu. Kitaev, Ann. Phys. **303**, 2 (2003).
- <sup>7</sup>S. Das Sarma, M. Freedman, and C. Nayak, Phys. Today **59** (7), 32 (2006).
- <sup>8</sup>C. Zhang, V. W. Scarola, S. Tewari, and S. Das Sarma, Proc. Natl. Acad. Sci. U.S.A. **104**, 18415 (2007); see also, J. Vidal, S. Dusuel, and K. P. Schmidt, arXiv:0801.4620 (unpublished); S. Dusuel, K. P. Schmidt, and J. Vidal, Phys. Rev. Lett. **100**,

- 177204 (2008); L. Jiang, Gavin K. Brennen, Alexey V. Gorshkov, Klemens Hammerer, Mohammad Hafezi, Eugene Demler, Mikhail D. Lukin, and Peter Zoller, Nat. Phys. **4**, 482 (2008); M. Aguado, G. K. Brennen, F. Verstraete, and J. I. Cirac, Phys. Rev. Lett. **101**, 260501 (2008).
- <sup>9</sup>L.-M. Duan, E. Demler, and M. D. Lukin, Phys. Rev. Lett. **91**, 090402 (2003).
- <sup>10</sup>A. Micheli, G. K. Brennen, and P. Zoller, Nat. Phys. **2**, 341 (2006).
- <sup>11</sup>H.-Q. Zhou and J. P. Barjaktarević, J. Phys. A: Math. Theor. **41**, 412001 (2008); H.-Q. Zhou, J.-H. Zhao, and B. Li, *ibid.* **41**, 492002 (2008); H.-Q. Zhou, arXiv:0704.2945 (unpublished).
- <sup>12</sup>H.-Q. Zhou, R. Orús, and G. Vidal, Phys. Rev. Lett. **100**, 080601 (2008).
- <sup>13</sup>H.-Q. Zhou, J.-H. Zhao, H.-L. Wang, and B. Li, arXiv:0711.4651 (unpublished).
- <sup>14</sup>H.-Q. Zhou, arXiv:0803.0585 (unpublished).

- <sup>15</sup>It is a difficult task to evaluate the ground state fidelity per site if a quantum lattice system is not exactly solvable. However, thanks to the latest advances in classical simulations of quantum lattice systems (Refs. 24–27), a practical way to compute it is now available using the tensor network algorithms for translationally invariant infinite-size quantum lattice systems (Ref. 12).
- <sup>16</sup>R. J. Baxter, arXiv:cond-mat/0611167 (unpublished).
- <sup>17</sup>Another fidelity approach to QPTs is based on the fidelity between two neighboring states, see P. Zanardi and N. Paunković, Phys. Rev. E **74**, 031123 (2006); For applications to various quantum lattice systems, see, e.g., P. Zanardi, M. Cozzini, and P. Giorda, arXiv:quant-ph/0606130 (unpublished); N. Oelkers and J. Links, Phys. Rev. B **75**, 115119 (2007); M. Cozzini, R. Ionicioiu, and P. Zanardi, arXiv:cond-mat/0611727 (unpublished); L. Campos Venuti and P. Zanardi, Phys. Rev. Lett. **99**, 095701 (2007); P. Buonsante and A. Vezzani, *ibid.* **98**, 110601 (2007); W.-L. You, Y.-W. Li, and S.-J. Gu, Phys. Rev. E **76**, 022101 (2007); S. Chen, L. Wang, S.-J. Gu, and Y. Wang, *ibid.* **76**, 061108 (2007); S. J. Gu, H. M. Kwok, W. Q. Ning, and H. Q. Lin, Phys. Rev. B **77**, 245109 (2008); Y. C. Tzeng and M. F. Yang, Phys. Rev. A **77**, 012311 (2008); S. Chen, L. Wang, Y. Hao, and Y. Wang, *ibid.* **77**, 032111 (2008); L. Campos Venuti, M. Cozzini, P. Buonsante, F. Massel, N. Bray-Ali, and P. Zanardi, Phys. Rev. B **78**, 115410 (2008).
- <sup>18</sup>M. F. Yang, Phys. Rev. B **76**, 180403(R) (2007); J. O. Fjærestad, J. Stat. Mech. 2008, P07011 (2008).
- <sup>19</sup>H.-D. Chen and Z. Nussinov, arXiv:cond-mat/0703633 (unpublished).
- <sup>20</sup>X.-Y. Feng, G.-M. Zhang, and T. Xiang, arXiv:cond-mat/0610626 (unpublished).
- <sup>21</sup>B. Roostaei, K. J. Mullen, and A. T. Rezakhani, Phys. Rev. B **78**, 075411 (2008).
- <sup>22</sup>H.-D. Chen and J. P. Hu, Phys. Rev. B **76**, 193101 (2007).
- <sup>23</sup>K. P. Schmidt, S. Dusuel, and J. Vidal, Phys. Rev. Lett. **100**, 057208 (2008).
- <sup>24</sup>G. Vidal, Phys. Rev. Lett. **98**, 070201 (2007).
- <sup>25</sup>J. Jordan, R. Orús, G. Vidal, F. Verstraete, and J. I. Cirac, Phys. Rev. Lett. **101**, 250602 (2008).
- <sup>26</sup>G. Vidal, Phys. Rev. Lett. **101**, 110501 (2008).
- <sup>27</sup>G. Vidal, Phys. Rev. Lett. **99**, 220405 (2007); G. Evenbly and G. Vidal, Phys. Rev. B **79**, 144108 (2009); arXiv:0710.0692.
- <sup>28</sup>This amounts to the statement that the fidelity per lattice site does not depend on which state has been chosen among degenerate states in the ground state subspace for a system with topological order. This has been shown for different states of the toric code (Ref. 31). That is, the tensor network representation for different states shares the same tensors except for their top tensor, where the relevant topological information is stored. Such a difference does not contribute to the fidelity per lattice site.
- <sup>29</sup>For generic  $J_x$ ,  $J_y$ , and  $J_z$ , we have  $k_1 = 1/(8\pi^2 J_x J_y)$ .
- <sup>30</sup>M. N. Barber, in *Phase Transitions and Critical Phenomena*, edited by C. Domb and J. L. Lebowitz (Academic, London, 1983), Vol. 8.
- <sup>31</sup>M. Aguado and G. Vidal, Phys. Rev. Lett. **100**, 070404 (2008).